

Murray R. Snyder, George Washington University,
Hyung Suk Kang, Johns Hopkins University Applied Physics Laboratory,
Cody J. Brownell and John S. Burks, United States Naval Academy

Validation of Ship Air Wake Simulations and Investigation of Ship Air Wake Impact on Rotary Wing Aircraft

ABSTRACT

This paper provides an update on a multi-year research project that involves the systematic investigation of ship air wakes using an instrumented research vessel. The object is to validate Computational Fluid Dynamics (CFD) tools that will be useful in determining ship air wake impact on rotary wing aircraft. Currently, ship launch and recovery wind limits and envelopes are primarily determined through at sea *in situ* flight testing that is expensive and frequently difficult to schedule and complete. The 108 ft long research vessel has been modified to include a flight deck and hangar-like structure to produce air wake data that is in the same order of magnitude as that from a modern destroyer. The research vessel is equipped with three-component ultrasonic anemometers to collect air wake data. Repeated underway testing has been performed to collect *in situ* data while wind tunnel testing has been also performed on a 4% scale model of the research vessel. Comparison of *in situ* data from above the flight deck with similar data from wind tunnel testing and CFD simulations shows good agreement in velocity direction for a headwind condition and for winds 15° and 30° off the starboard bow. Off-ship air turbulence data collected with an instrumented radio controlled helicopter shows that an off-ship air wake is present where predicted by CFD simulations. Analysis indicates that CFD simulations likely require modeling of the atmospheric boundary layer to improve simulation accuracy.

NOTATION

CAD = Computer Aided Design

CFD = Computational Fluid Dynamics
IMU = Inertial Measurement Unit
LHA = Amphibious Assault Ship
MILES = Monotone Integrated Large Eddy Simulation
USNA = United States Naval Academy
YP = Patrol Craft, Training
 β = relative wind angle on horizontal plane
 H = height of hangar structure
 x = distance aft of hangar
 y = distance port or starboard of centerline
 z = distance above flight deck
 u_{fit} = least-square curve fit of boundary layer
 U_R = bow reference anemometer velocity
 U_{YP} = YP velocity

INTRODUCTION

Launch and recovery of rotary wing aircraft from naval vessels can be very challenging and potentially hazardous. Ship motion combined with the turbulence that is created as the wind flows over the ship's superstructure can result in rapidly changing flow conditions for rotary wing aircraft. Additionally, dynamic interface effects between the vessel air wake and the rotor wake are also problematic.

To ensure aircraft and vessel safety, launch and recovery envelopes are prescribed for specific aircraft types on different ship classes (Figure 1).¹ Permissible launch and recovery envelopes are often restrictive because of limited flight envelope expansion. Flight testing required to expand the envelopes is frequently difficult to schedule, expensive and potentially hazardous. Currently, the launch and recovery wind limits and air operation envelopes are primarily

determined via the subjective analysis of test pilots (e.g. excessive flight control inputs are required to safely land on the flight deck), using a time consuming and potentially risky iterative flight test build-up approach. The time and risk of flight testing could be reduced through the complementary use of computational tools to predict test conditions and extrapolate test results, thereby reducing the number of actual flight test points required. However, current computational methods are insufficiently validated for ships with a complex superstructure, such as a destroyer or cruiser.²⁻⁹ Validated computational air wake predictions can also be used for ship design and operational safety analysis.

and the associated human subjective analysis associated with flight testing. Rather, we hope to develop validated CFD tools that will allow a reduction in the amount of flight testing required and to focus the flight testing that is performed on the limits of the launch and recovery envelopes where pilot subjective analysis is particularly important.

This research project leverages unique resources available at the United States Naval Academy (USNA) that allow for a systematic analysis of ship air wakes.

IN SITU WAKE MEASUREMENT

USNA operates a fleet of YP (Patrol Craft, Training) vessels for midshipman training. The USNA YPs (Figure 2) are relatively large vessels (length of 108 ft (32.9 m) and an above waterline height of 24 ft (7.3m)) with a superstructure and deck configuration that resembles that of a modern destroyer or cruiser. The size of the YPs is such that air wake data can be collected with Reynolds numbers in the same order of magnitude as those for modern naval warships, an important consideration in aerodynamic modeling. (Reynolds number is the ratio of inertia forces to viscous forces.) As shown in Figure 3, YP676 has been modified to add a flight deck and hangar-like structure similar to those on modern US Navy ships.

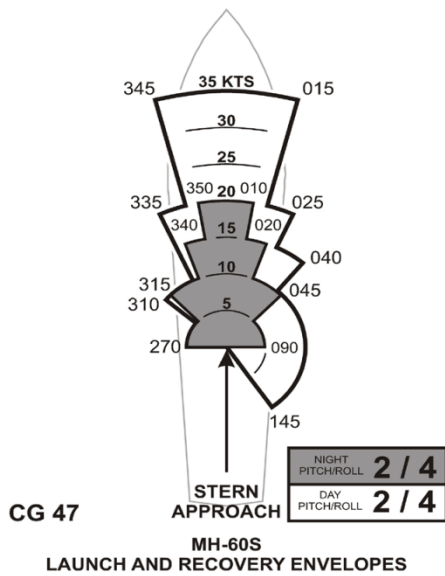


Figure 1. Launch and recovery envelopes, showing allowable relative wind over deck, for MH-60S helicopters on USS Ticonderoga (CG 47) class cruiser (Ref. 1).

This paper presents an update of a multi-year project to develop and validate Computational Fluid Dynamics (CFD) tools to reduce the amount of at-sea *in situ* flight testing required and make rotary wing launch and recovery envelope expansion safer, more efficient, and affordable. The authors do not envision these CFD tools as replacing the need for flight testing



Figure 2. USNA YP676.



Figure 3. Detail of YP676 flight deck and hangar-like structure.

Ultrasonic anemometers have been installed to allow for direct measurement of wind velocities over the flight deck (Figure 4). The anemometers are the Applied Technology Inc. “A” style three-velocity component model with a 5.91 inch path length and a measurement accuracy of ± 1.18 inch/s. The anemometers are connected to a synchronizer that allows up to 8 different anemometers to be sampled simultaneously up to 20 Hz, which is the sample rate for the current measurements. As of the submission of this paper, over 45 underway test periods in the Chesapeake Bay have been completed. Air wake velocity data have been collected at 162 points between 16.5 and 83 inches above the flight deck for winds up to 17 knots (nautical mile/hr) for three different incoming flow conditions, i.e., a head wind condition and winds 15° and 30° off the starboard bow.



Figure 4. Ultrasonic anemometers installed on YP676 flight deck.

Underway test periods in the Chesapeake Bay last typically 6 to 8 hours and include 5 or 6 data collection periods of 20-30 minutes at a specified incoming relative wind condition. Weather conditions can vary widely with typical sea state of 3 or less (with a maximum observed wave height of approximately 4 feet (1.2 m)). During underway data collection periods, real time data output from the reference anemometer (third from bottom of Figure 5) is continuously monitored to ensure desired relative wind is approximately maintained and that data quality is satisfactory. This information is also displayed on the YP’s bridge such that the ship’s helmsman can take corrective action to adjust ship heading. Furthermore, only data that are collected within $\pm 5^\circ$ of the desired wind over deck angle β is used for comparison with wind tunnel and CFD results.



Figure 5. Bow anemometer array. Reference anemometer is third from bottom.

WIND TUNNEL MEASUREMENTS

Wind tunnel tests of a 4% scale model of the YP were completed in USNA's recirculating wind tunnel (with a test section of 42-inch in height \times 60-inch in width \times 120-inch in length) in November 2010. Figure 6 shows the YP model in the wind tunnel with the 18 hole Omniprobe that is used to collect three-dimensional velocity data over the flight deck and adjacent areas.

The wind tunnel tests were conducted at a test section free stream velocity of 300 ft/s to match the Reynolds number of the YP experiencing a 7 knot relative wind. (The Reynolds numbers based upon ship length under these conditions is approximately 7.8×10^6 .) Velocity data were collected at 1855 points above and around the model flight deck for a fixed incoming velocity.



Figure 6. 4% scale YP model in USNA wind tunnel.

NUMERICAL SIMULATIONS

Advanced CFD simulations have been performed by USNA midshipmen using Cobalt,¹⁰ a commercial parallel processing CFD code which uses an unstructured tetrahedral grid system. As shown in Figure 7, the unstructured grid allows for finer resolution near boundaries and in other regions where more complicated flow structures are expected.

The tetrahedral grids are divided into partitions to allow parallel processing on advanced computer clusters. Such partitioning speeds up the solution generation by allowing an individual processor to solve the flow field in a limited number of tetrahedra.

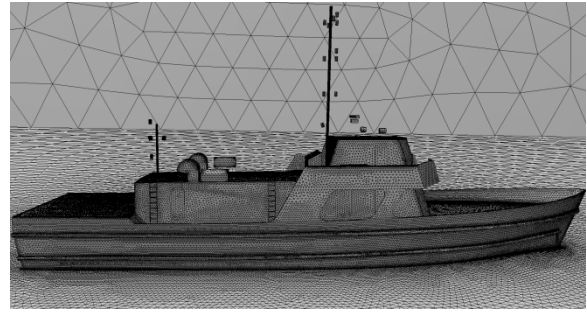


Figure 7. Unstructured surface grid.

Midshipmen have performed CFD analysis for both 7 and 20 knots of relative wind. CFD simulations, using an unstructured grid system of approximately 15.5 million tetrahedra, have been completed for a head wind and for winds from the starboard bow (or relative wind angle β) of 15°, 30°, 45°, 60°, 75° and 90°. These analyses used a Monotone Integrated Large Eddy Simulation (MILES), which is a laminar, time accurate flow model.¹¹ In a study involving an LHA Class US Navy ship, the MILES approach has been shown to correctly predict dominant frequencies in the measured flow field during *in situ* testing with four anemometers installed on the flight deck and in concurrent 1/120th scale model wind tunnel testing.¹²

SIGNIFICANT RESULTS

The following significant conclusions,¹³⁻²¹ have been previously provided:

1. Initial CFD analysis done in the summer of 2009 on an unmodified YP model was useful in determination of sensor placement on the modified YP676.
2. As one would expect, turbulent kinetic energy is significantly greater in the superstructure wake than in the free stream flow observed by the bow reference anemometer.
3. Minor ship pitch and roll motions, as measured by an installed inertial measurement unit (IMU), have negligible impact on the mean velocity fields in the air wake.

4. Spatial velocity correlations show, as predicted by CFD analysis, a distinctive shear layer present aft of the hangar-like superstructure with the largest scale turbulent eddy which is approximately the same size as the height of the superstructure. A similar shear layer with associated recirculation zone has also been observed in flow visualizations with fog generators.

5. CFD simulations and *in situ* measurements at the bow reference anemometer location show good agreement for the induced vertical velocity component arising from ship interference effects.

6. Over numerous underway test periods, good measurement repeatability has been consistently observed.²¹

7. As shown in Figures 8 to 15, for $\beta=0^\circ$, $\beta=15^\circ$ and $\beta=30^\circ$, there is good agreement in velocity direction between collected *in situ* and wind tunnel data with CFD flow simulations, with, on average, less than 15° difference between the three data sets. (In Figures 8 to 13 the black arrows represent the scaled *in situ* data, the red arrows represent scaled wind tunnel data and blue arrows represent the CFD data. Locations with two black arrows represent *in situ* data collected on different underway test periods at the same sampling location. U_R represents the flow direction and scaled magnitude in the horizontal plane observed at the bow reference anemometer. $H = 1.5$ m is the height of the hangar above the flight deck, x represents the distance aft of the hangar, y represents athwartships offset from the fore to aft centerline of the ship and z represents vertical distance above the flight deck.)

8. Velocity magnitude differences between the three data sources, however, are greater than direction differences, with the most likely source of the observed magnitude disparities resulting from the fact that CFD simulations and wind tunnel experimentation do not currently model the atmospheric boundary layer encountered by the full size ship.

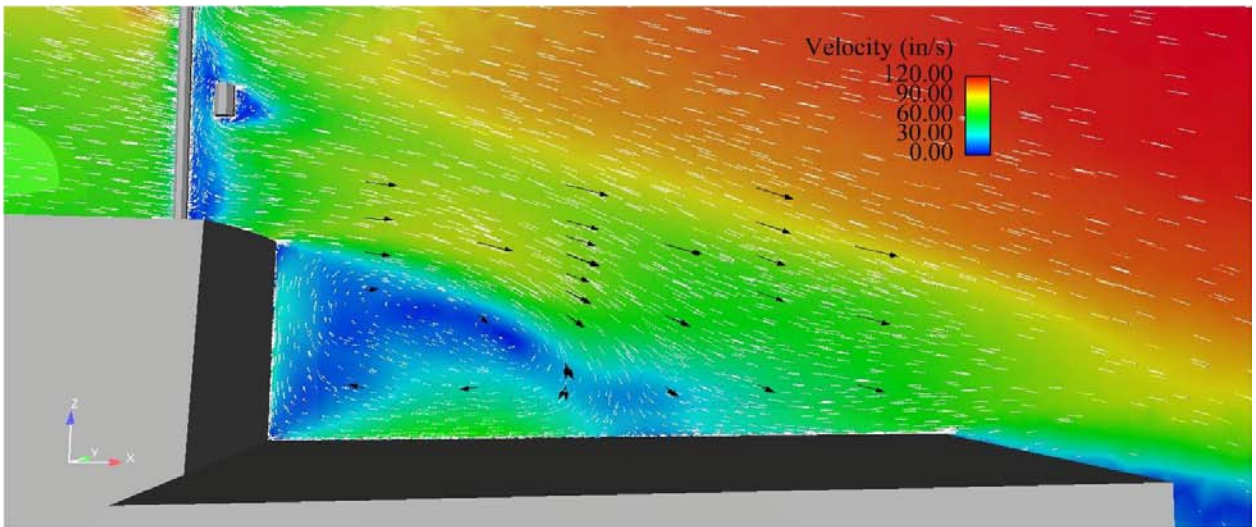


Figure 8. Scaled *in situ* data (black arrows) vs. 7 knot CFD simulations (white arrows and color contours) for headwind ($\beta = 0^\circ$) at centerline of the flight deck (7 knots = 141 in/s). Locations with multiple black arrows are where data was taken on different days.

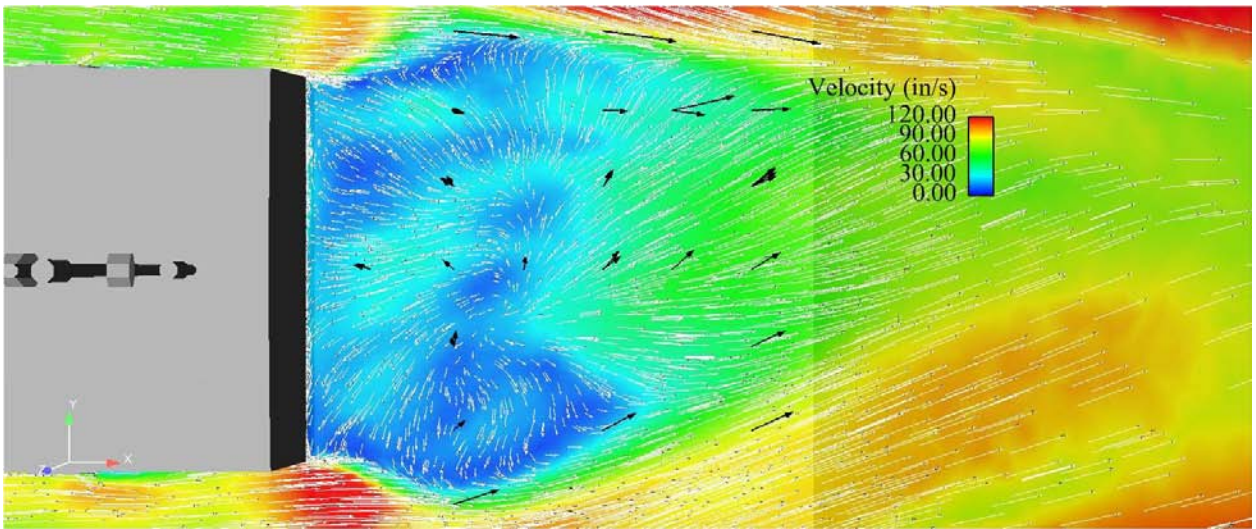


Figure 9. Scaled *in situ* data (black arrows) vs. 7 knot CFD simulations (white arrows and color contours) for relative wind $\beta = 15^\circ$ for the horizontal plane 17 inches above the flight deck (7 knots = 141 in/s). Locations with multiple black arrows are where data was taken on different days.

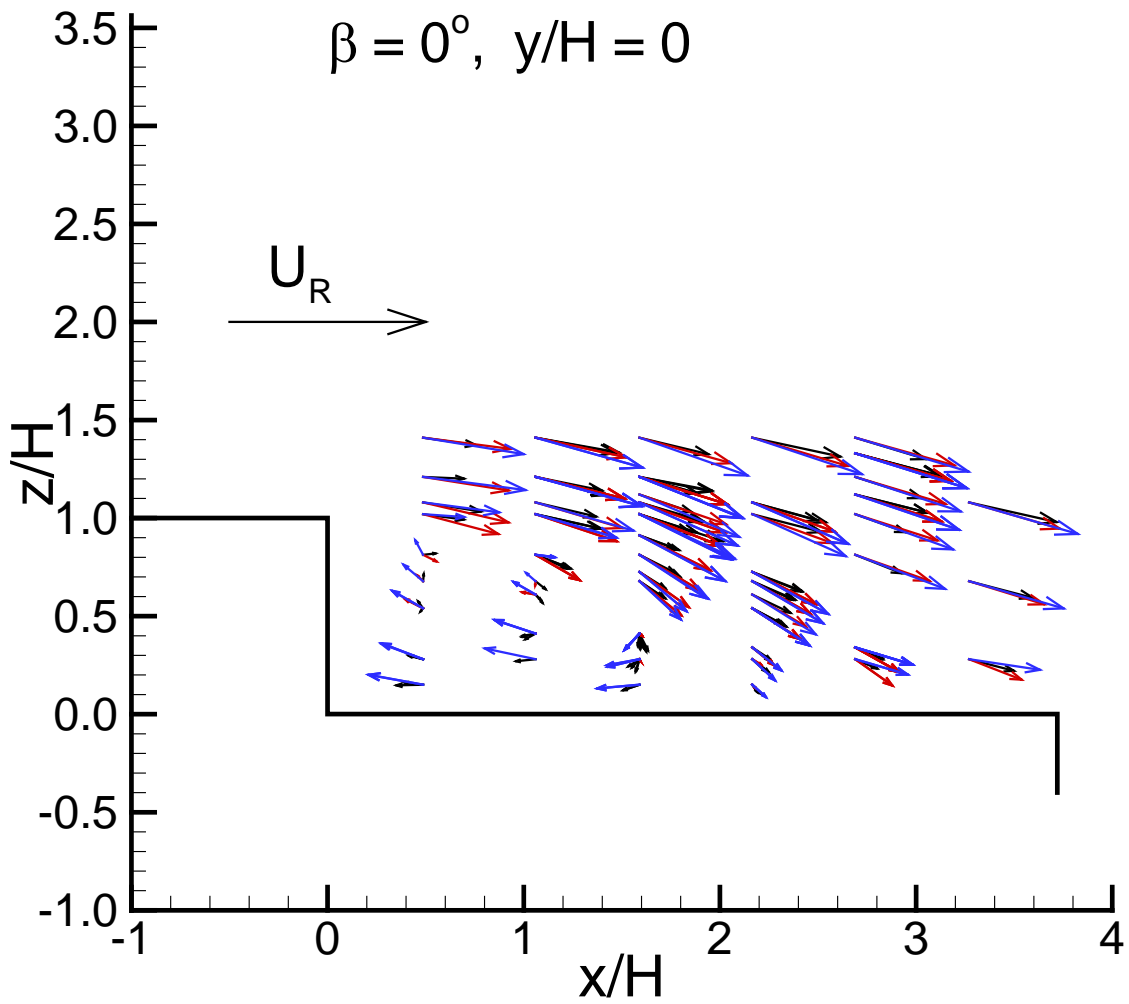


Figure 10. Centerline vertical plane ($y/H = 0$) for a headwind (black arrows are *in situ* data, red arrows are wind tunnel data and blue arrows are CFD data).

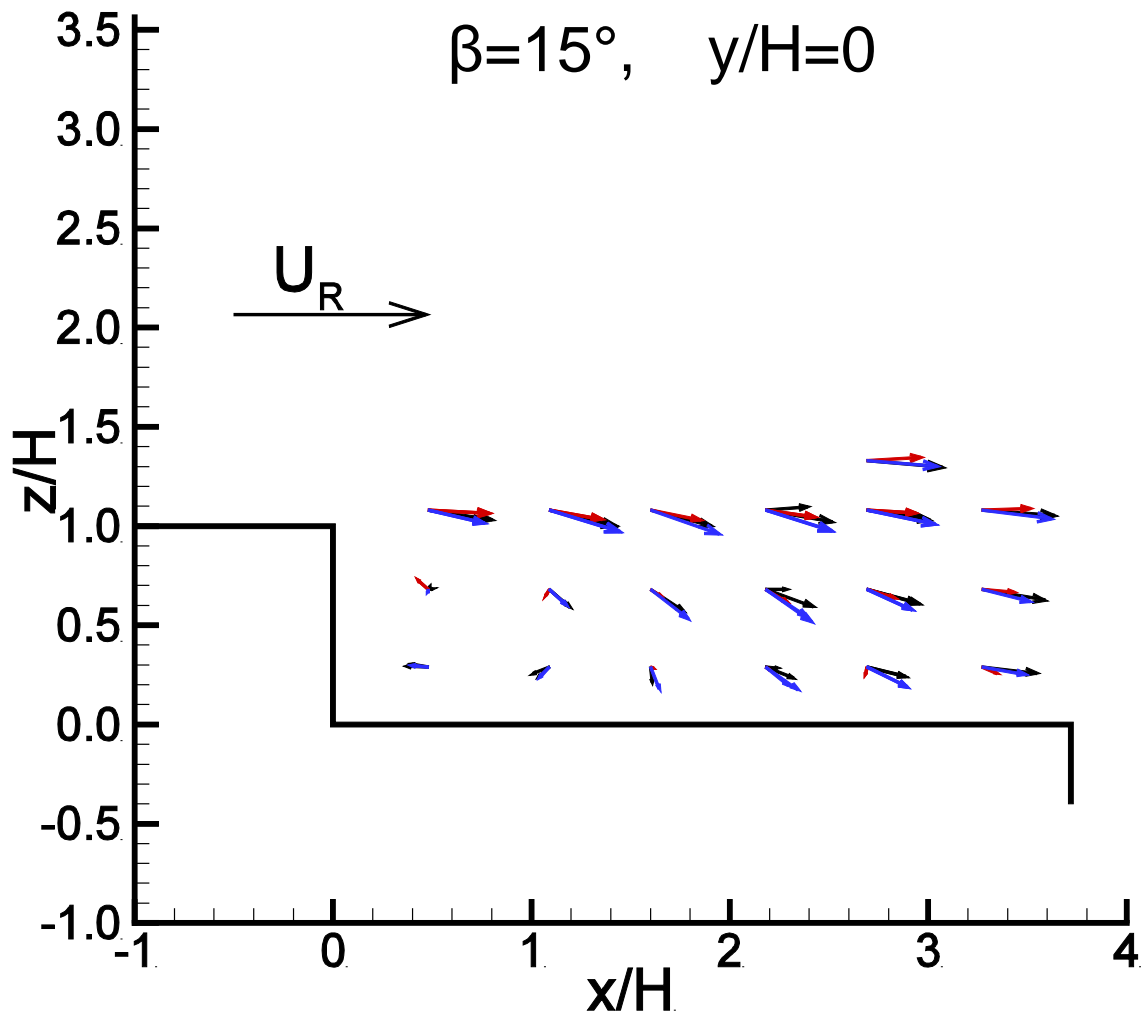


Figure 11. Centerline vertical plane ($y/H = 0$) for relative wind $\beta = 15^\circ$ (black arrows are *in situ* data, red arrows are wind tunnel data and blue arrows are CFD data).

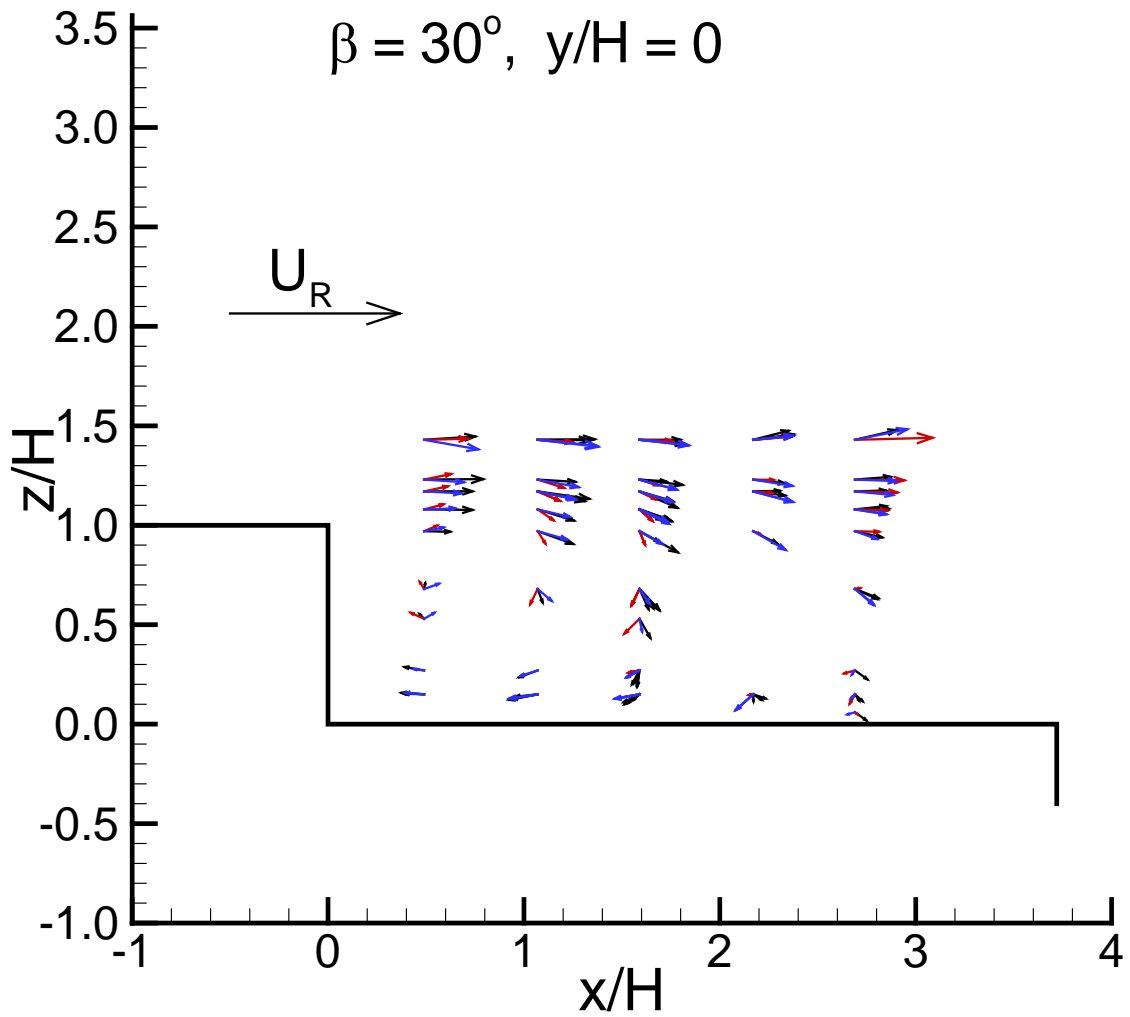


Figure 12. Centerline vertical plane ($y/H = 0$) for relative wind $\beta = 30^\circ$ (black arrows are *in situ*, red arrows are wind tunnel data and blue arrows are CFD data).

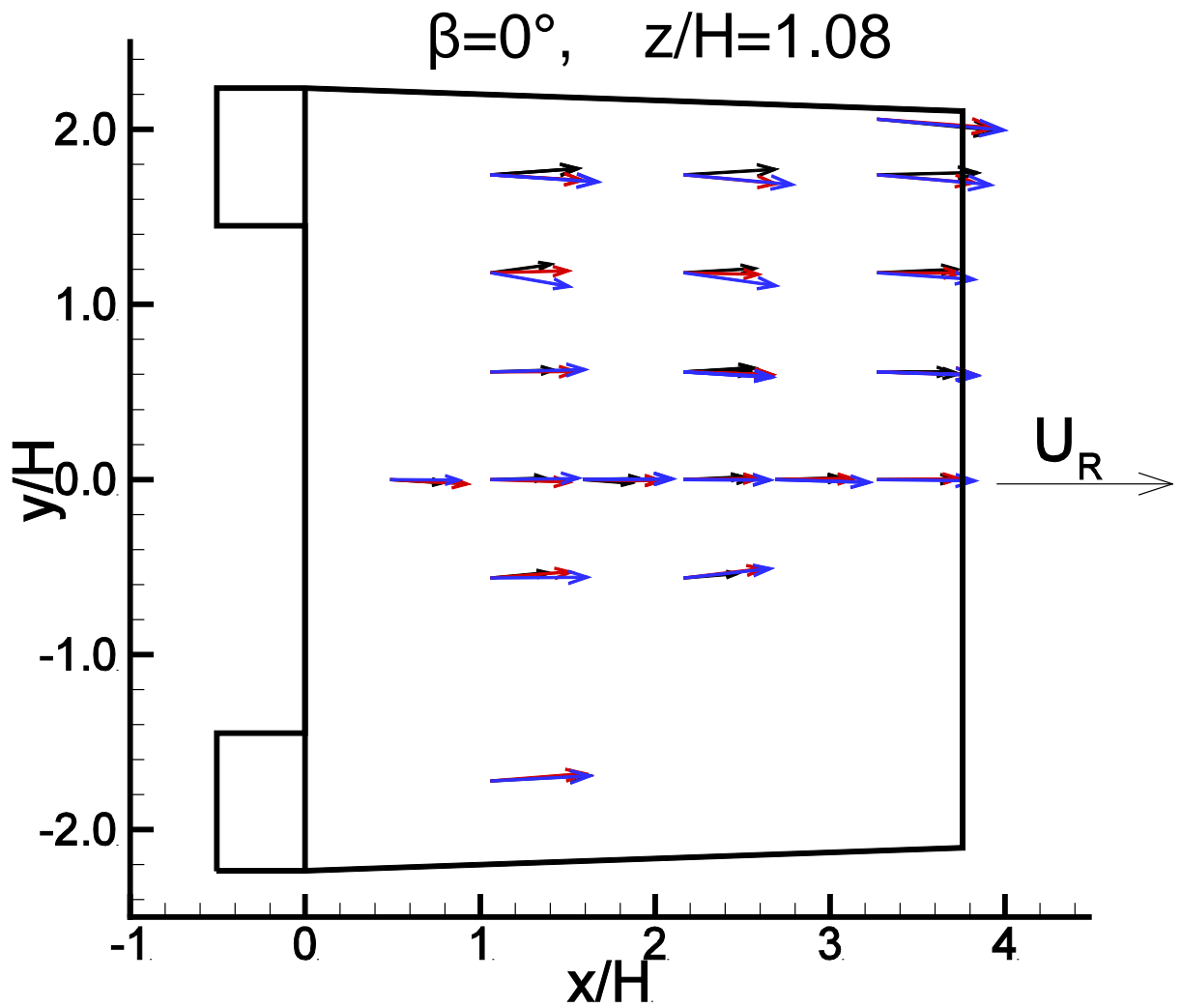


Figure 13. Horizontal vertical plane $z/H = 1.08$ (63.7 inches) above the flight deck for a headwind (black arrows are *in situ* data, red arrows are wind tunnel data and blue arrows are CFD data).

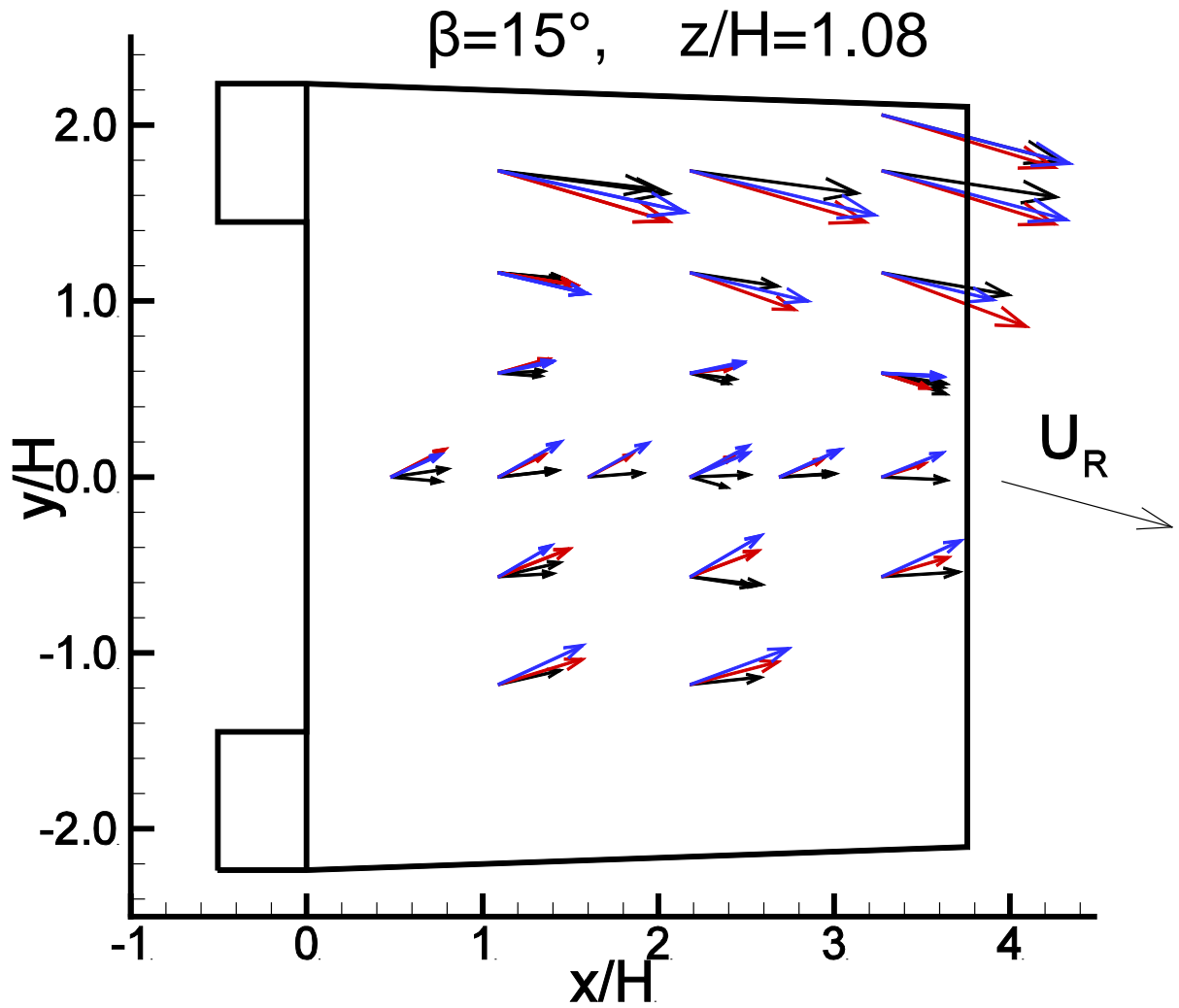


Figure 14. Horizontal vertical plane $z/H = 1.08$ (63.7 inches) above the flight deck for relative wind $\beta = 15^\circ$ (black arrows are *in situ* data, red arrows are wind tunnel data and blue arrows are CFD data).

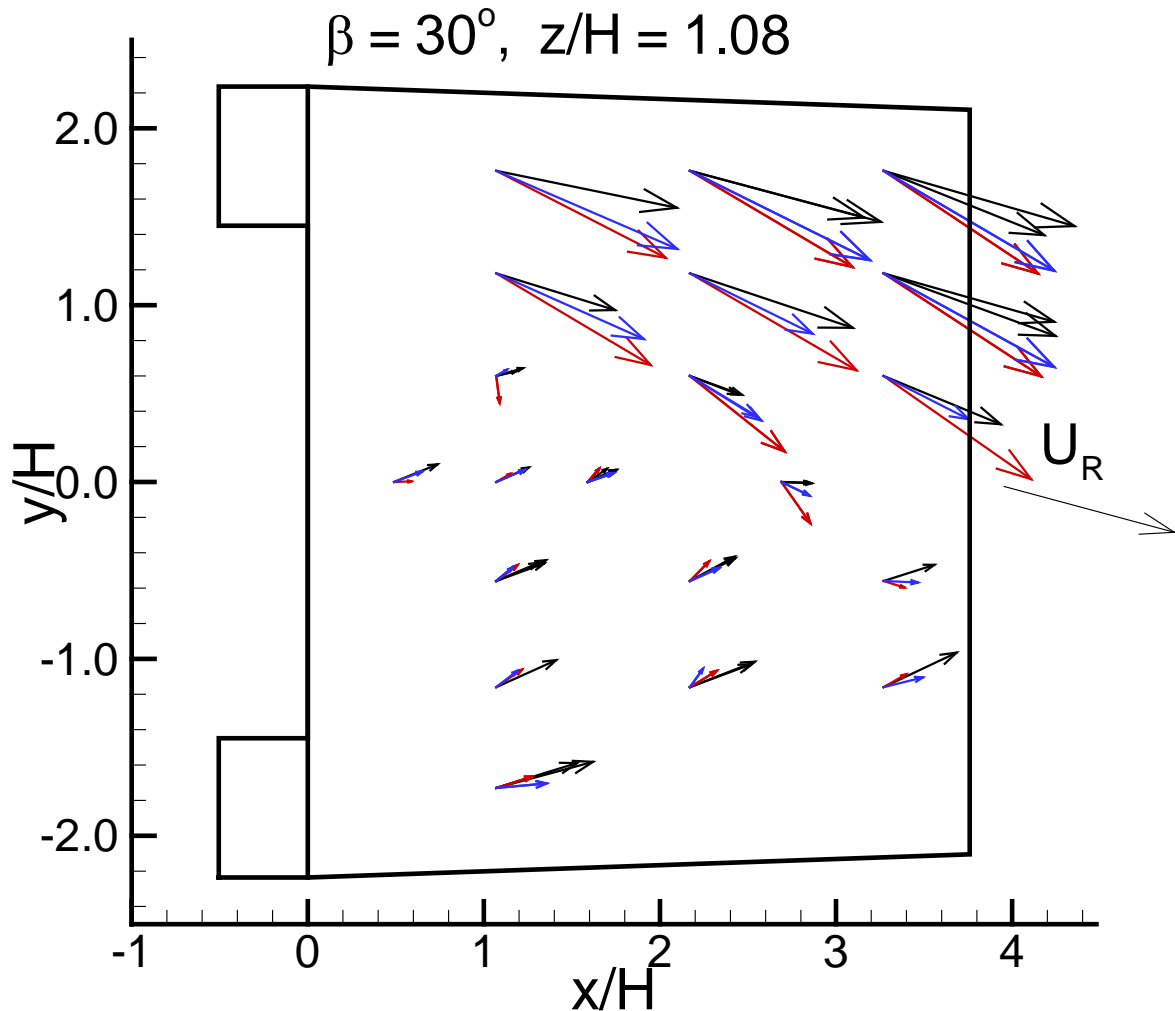


Figure 15. Horizontal vertical plane $z/H = 1.08$ (63.7 inches above the flight deck) for relative wind $\beta = 30^\circ$ (black arrows are *in situ* data, red arrows are wind tunnel data and blue arrows are CFD).

9. A small remotely piloted helicopter, shown in Figure 16, has been used to identify the turbulent air wake region aft of the YP676 flight deck.^{22,23} As the helicopter, which has a 4.5 ft diameter rotor, was maneuvered through regions in the ship's air wake where there are steep velocity gradients, an IMU mounted on the helicopter recorded noticeable unsteadiness in the helicopter's flight path. Concurrently, the relative position of the helicopter was determined by comparing the GPS derived position of the helicopter with that of a reference

position on the ship. Combining these two measurement systems, the locations of sharp gradients in the air wake were mapped relative to the ship (accurate within one rotor diameter of the helicopter) and compared with CFD simulations of similar wind-over-deck configurations.

When the helicopter encountered the ship air wake there would be a noticeable increase in flight path unsteadiness, as measured by the IMU, due to interaction with the air wake.²³

These interactions were compared with CFD predictions of the ship air wake with the relative position determined through use of GPS receivers on both the ship and helicopter. Relative position was determined to be accurate within one meter (approximately 3 ft),²³ which is slightly smaller than the length scale of the main rotor of the helicopter.



Figure 16. Radio controlled instrumented helicopter flying astern of YP676 in the Chesapeake Bay

Figures 17 and 18, respectively, show helicopter flight paths along which increased unsteadiness was observed superimposed over CFD air wake predictions for both $\beta = 15^\circ$ and 30° . Figures 17 and 18 show good correlation between the location of the YP's air wake from the CFD simulations versus what was measured by the IMU onboard the helicopter during underway testing.

During underway flight operations the YP's craft master attempted to keep a constant wind over deck condition based upon the reference anemometer. Since winds typically shift during a given flight, with increasing β most common, the craft master had to adjust ship's course to maintain an approximately constant wind over deck. Shifting winds with subsequent adjustment in ship's course explains the apparent drift of the measured wake towards the port side further aft of the flight deck.

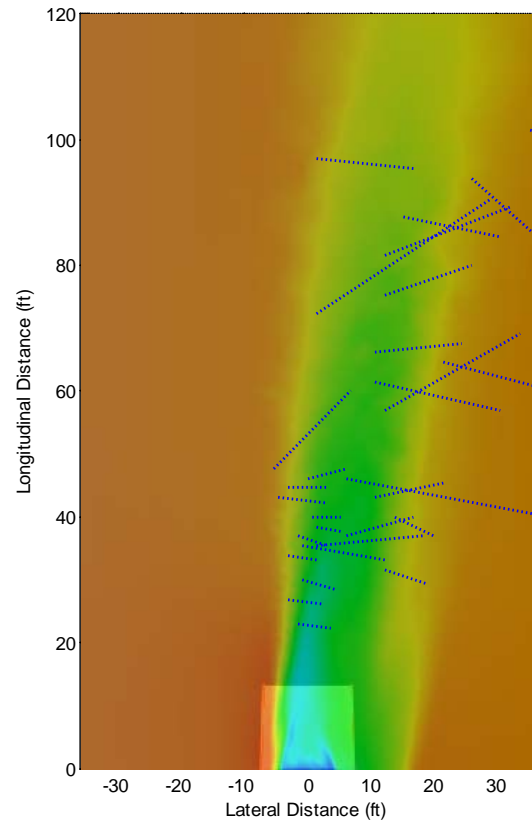


Figure 17. Measured air wake location (blue dashed lines) and CFD simulation (colored background) for $\beta=15^\circ$ at the top of the hangar structure.

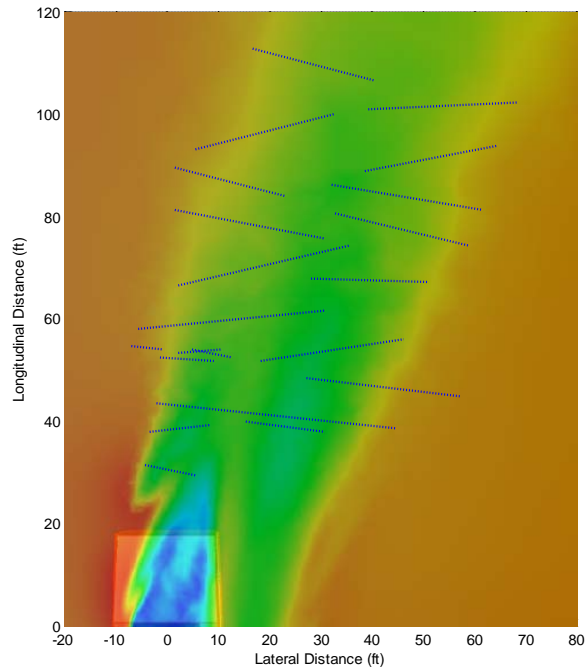


Figure 18. Measured air wake location (blue dashed lines) and CFD simulation (colored background) for $\beta=30^\circ$ at the top of the hangar structure.

10. There are significant velocity magnitude deviations between the CFD simulations, which assume a uniform velocity profile from the ocean surface upward, and with the atmospheric boundary layer measured during a July 2011 underway. In Figure 19 the fitted power-law velocity profile ($u_{fit} + U_{YP}$)/ U_{Bow} (red line) of underway data is compared with that from CFD simulations (blue line). u_{fit} was determined using a least squares curve fitting, $u_{fit} = a(z/b)^m + c$, where $a = 3.83$, $b = 4.84$, $c = 0.05$, $m = 0.351$ are constants and z is the distance above the waterline. The reference bow anemometer (third anemometer from the bottom of Figure 5) location is shown with the horizontal green line. Thus, u/U_{Bow} is 1 at the reference bow anemometer height of 5.58 m. The contribution of the YP speed to u/U_{Bow} is 46.4%. The decrease of the CFD velocity near $z = 3$ m is attributed to YP hull shape effects on the incoming flow. Though the velocity magnitude is matched near the bow height, the incoming velocity profile imposed in CFD simulations is uniform ($u/U_{Bow} \sim 1$), which is quite different

from the measured mean velocity profile (red line) of the actual atmospheric boundary layer. These results emphasize the importance of including an atmospheric boundary layer profile in CFD simulations.

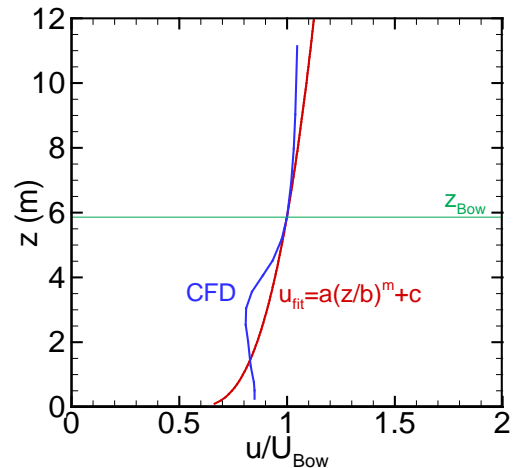


Figure 19: Fitted power law velocity profile (red line) of underway anemometer data vs. CFD velocity profile (blue line). The green line is the height of the bow reference anemometer. (a , b , c and m are constants determined through least-square curve fitting, z is the distance above the vessel's waterline, and u_{fit} is the fitted velocity.)

RECENT BOUNDARY LAYER MEASUREMENTS

Figure 20 shows the fitted power law velocity profile collected during an underway in May 2012. In this figure the horizontal velocity component (square root of the squares of the x and y direction velocity components, $\sqrt{u^2 + v^2}$) is plotted vs. elevation in dimensional form. Unlike in Figure 19, the ship speed U_{YP} was subtracted from the x -component. For a least squares fit a zero-velocity data point was added at the sea surface. In this case the least squares fit, $u_{fit} = a(z/b)^m + c$, gives $a = 1.06$, $b = 3.24$, $c = 0$ and $m = 0.58$. For this fit there is a residual $R = 0.972$.

The difference between the experimentally observed atmospheric boundary layers shown in Figures 19 and 20 suggest, not unexpectedly, the highly variable nature of the atmospheric

boundary layer observed over the Chesapeake Bay.

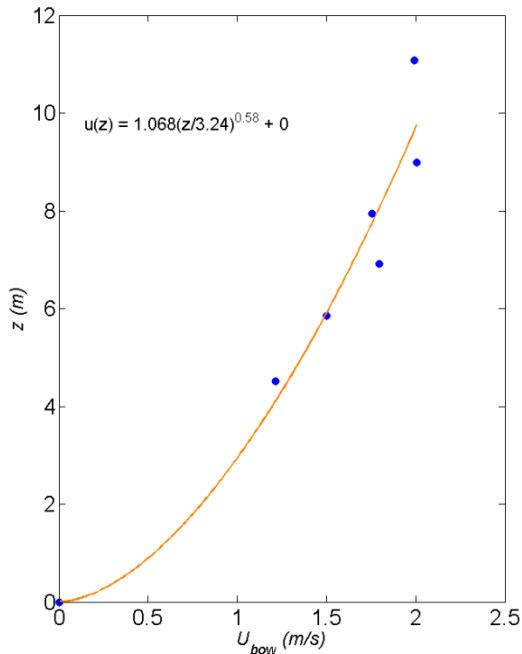


Figure 20. Atmospheric boundary layer observed during May 2012 underway testing. A least squares fit of horizontal velocity, less ship velocity U_{VP} , is shown.

CFD GRID SENSITIVITY STUDY

During the summer of 2012 Midshipmen interns completed a CFD grid sensitivity study for 17 and 22 million tetrahedra. As shown graphically in Figure 21, no significant difference was noted between the two simulations.

CONCLUSIONS

Extensive data collection has shown velocity direction agreement between collected *in situ* and wind tunnel data with CFD flow simulations for $\beta = 0^\circ$, 15° and 30° relative winds above the YP flight deck. For all three data sets, however, there are disparities in velocity magnitudes that may result from the fact that the CFD simulations and wind tunnel experimentation do not model the atmospheric boundary layer encountered by the full size ship.¹⁹ Additional atmospheric boundary layer data encountered during subsequent testing is provided in this paper. The atmospheric boundary layers

observed on different days were noted to vary significantly. (Other possible sources of the velocity magnitude discrepancies include using the MILES approach with the associated laminar boundary layer, the use of tetrahedral grids inside the boundary layer, and the variable nature of the wind speed and direction encountered during underway testing.) Finally, the detection of CFD predicted off-ship air wakes has been performed through the use of an IMU equipped small remote controlled helicopter.

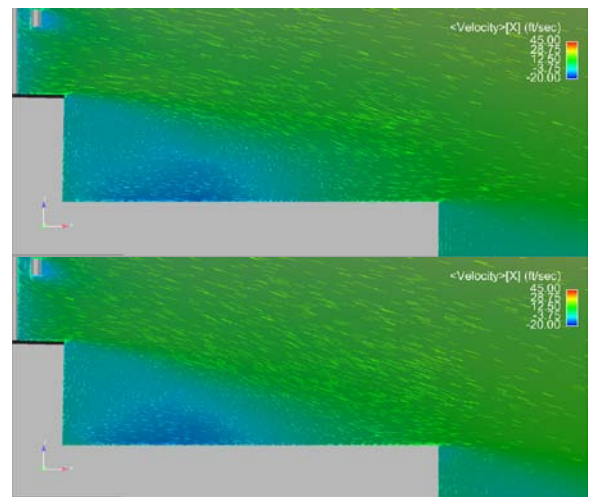


Figure 21. Comparison of CFD simulations for $\beta = 0^\circ$. Top is grid with 17 million tetrahedrons while bottom is grid with 22 million tetrahedra.

FUTURE WORK

Additional effort will be required to develop validated CFD tools that would be useful in determination of rotary wing launch and recovery envelopes. Specific areas which we will investigate in the future include:

1. Collect additional *in situ* data above the flight deck for more off-axis wind conditions, specifically $\beta = 45^\circ$ and 90° data. Comparisons will also be made between *in situ* data and CFD simulations for $\beta = 45^\circ$ and 90° . Wind tunnel data for $\beta > 30^\circ$ are not obtainable due to blockage effects.
2. Collect *in situ* data for the immediate region around but outside the flight deck. Data in

regions within 5-6 feet of the flight deck will be collected through the use of anemometers whereas more distant regions will require alternative sampling techniques such as laser-based instruments or through an unmanned helicopter equipped with air data sensors.

3. Collect extensive atmospheric boundary layer data to quantify the average boundary layer velocity profile encountered during underway testing. This average boundary layer will then be modeled in updated CFD simulations and in wind tunnel testing to see if a closer match can be obtained in flow velocity magnitude.

4. A wind tunnel Reynolds number sensitivity study will be performed to determine if ship air wake correlations developed using matched Reynolds numbers between *in situ* and wind tunnel testing can be extended to cases where it is not possible to match Reynolds numbers in wind tunnel testing (e.g. wind tunnel testing of a 1% or smaller ship model).

5. Investigate passive modification of ship air wakes previously studied by Shafer.²⁴ During the summer of 2012 YP676 was modified with the addition of flow control fences as shown in Figures 22 and 23. Underway *in situ* and wind tunnel data for the modified vessel will be collected and compared with CFD simulations to see if ship air wake changes can be predicted numerically and whether flow control fences or similar designs could reduce the severity of ship air wake impact on rotary wing aircraft.

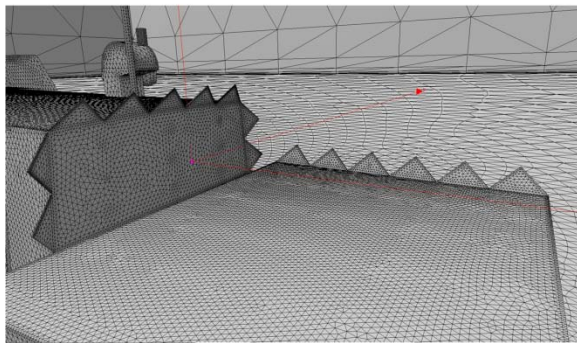


Figure 22. CFD grid showing flow control fences added to the top, port and starboard sides of hangar structure and starboard side of flight deck.



Figure 23. Flow control fences added starboard side of YP676 flight deck.

6. Perform additional CFD simulations using a structured prismatic grid vice the tetrahedral unstructured grid and with a turbulent boundary layer model (prior simulations used a laminar boundary layer). Also, since ship *in situ* data is collected with a $\beta \pm 5^\circ$ tolerance, additional simulations will be performed to investigate the effect of this tolerance on CFD results.

7. Dynamic interface, or the interaction between the ship air wake and the down wash from a rotary wing aircraft, will be investigated using a fixed flight deck mounted rotor of approximately 12 ft. diameter. Experimental data will be compared with additional advanced computer simulations.

References

¹“Helicopter operating procedures for air-capable ships NATOPS manual,” NAVAIR 00-08T-122, 2003.

²Guillot, M.J. and Walker, M.A., “Unsteady analysis of the air wake over the LPD-16,” *AIAA 2000-4125: 18th Applied Aerodynamics Conference*, Denver, Colorado, 2000.

³Guillot, M.J., “Computational simulation of the air wake over a naval transport vessel,” *AIAA Journal*, Vol. 40, No. 10, 2002, pp. 2130-2133.

⁴Lee, D., Horn, J.F., Sezer-Uzol, N., and Long, L.N., “Simulation of pilot control activity during helicopter shipboard operations,” *AIAA 2003-5306: Atmospheric Flight Mechanics Conference and Exhibit*, Austin, Texas, 2003.

- ⁵Carico, D., "Rotorcraft shipboard flight test analytic options," *Proceedings 2004 Institute of Electrical and Electronics Engineers (IEEE) Aerospace Conference*, Vol. 5, Big Sky, Montana, 2004.
- ⁶Lee, D., Sezer-Uzol, N., Horn, J.F., and Long, L.N., "Simulation of helicopter ship-board launch and recovery with time-accurate airwakes," *Journal of Aircraft*, Vol. 42, No. 2, 2005, pp. 448-461.
- ⁷Geder, J., Ramamurti, R. and Sandberg, W.C., "Ship airwake correlation analysis for the San Antonio Class Transport dock Vessel," Naval Research Laboratory paper MRL/MR/6410-09-9127, May 2008.
- ⁸Polsky, S., Imber, R., Czerwiec, R., & Ghee, T., "A Computational and Experimental Determination of the Air Flow Around the Landing Deck of a US Navy Destroyer (DDG): Part II," *AIAA-2007-4484: 37th AIAA Fluid Dynamics Conference and Exhibit*, Miami, Florida, 2007.
- ⁹Roper, D. M., Owen, I., Padfield, G.D. and Hodje, S.J., "Integrating CFD and pilot simulations to quantify ship-helicopter operating limits," *Aeronautical Journal*, Vol. 110, No. 1109, 2006, pp. 419-428.
- ¹⁰Strang, W.Z., Tomaro, R.F., and Grismer, M.J., "The Defining Methods of Cobalt60: A Parallel, Implicit, Unstructured Euler/Navier-Stokes Flow Solver," *AIAA-99-0786: 37th Aerospace Sciences Meeting and Exhibit*, Reno, Nevada, January 1999.
- ¹¹Boris, J., Grinstein, F., Oran, E., Kolbe, R., "New Insights into Large Eddy Simulation," *Fluid Dynamics Research*, Vol. 10, 1992, pp.199-228.
- ¹²Polsky, S.A., "A Computational Study of Unsteady Ship Airwake," *AIAA 2002-1022: 40th AIAA Aerospace Sciences Meeting and Exhibit*, Reno, Nevada, 2002.
- ¹³Snyder, M.R., et al., "Determination of Shipborne Helicopter Launch and Recovery Limitations Using Computational Fluid Dynamics," *American Helicopter Society 66th Annual Forum*, Phoenix, Arizona, 2010.
- ¹⁴Snyder, M.R., et al., "Comparison of Experimental and Computational Ship Air Wakes for YP Class Patrol Craft," *American Society of Naval Engineers Launch and Recovery Symposium*, Arlington, VA, December 2010.
- ¹⁵Snyder, M.R., Kang, H.S., Brownell, C.J., Luznik, L., Miklosovic, D.S., Burks, J.S. and Wilkinson, C.H., "USNA Ship Air Wake Program Overview," *AIAA 2011-3153: 29th AIAA Applied Aerodynamics Conference*, Honolulu, Hawaii, June 2011.
- ¹⁶Roberson, F.D., Kang, H.S. and Snyder, M.R., "Ship air wake CFD comparisons to wind tunnel and YP boat results," *AIAA 2011-3156: 29th AIAA Applied Aerodynamics Conference*, Honolulu, Hawaii, June 2011.
- ¹⁷Miklosovic, D.S., Kang, H.S. and Snyder, M.R., "Ship Air Wake Wind Tunnel Test Results," *AIAA 2011-3155: 29th AIAA Applied Aerodynamics Conference*, Honolulu, Hawaii, June 2011.
- ¹⁸Snyder, M.R. and Kang, H.S., "Comparison of Experimental, Wind Tunnel and Computational Ship Air Wakes for YP Class Patrol Craft," *AIAA-2011-058: 6th Ankara International Aerospace Conference*, Ankara, Turkey, September 2011.
- ¹⁹Snyder, M.R. and Kang, H.S., "Comparison of Experimental and Computational Ship Air Wakes for YP Class Patrol Craft," *AIAA 2011-7045: Centennial of Naval Aviation Forum*, Virginia Beach, Virginia, September 2011.
- ²⁰Snyder, M.R., Kang, H.S. and Burks, J.S., "Comparison of Experimental and Computational Ship Air Wakes for a Naval Research Vessel," *AIAA 2012-2897: 30th Applied Aerodynamics Conference*, New Orleans, Louisiana, June 2012.
- ²¹Brownell, C.J., Luznik, L., Snyder, M.R., Kang, H.S., and Wilkinson, C.H., "In situ air velocity measurements in the near wake of a ship superstructure," *Journal of Aircraft*, Vol. 49, No. 5, September—October 2012.
- ²²Metzger, J.D., Snyder, M.R., Burks, J.S. and Kang, H.S., "Measurement of Ship Air Wake Impact on a Remotely Piloted Aerial Vehicle," *American Helicopter Society 68th Annual Forum*, Fort Worth, Texas, May 2012.

²³Metzger, J.D., "Measurement of Ship Air Wake Impact on a Remotely Piloted Aerial Vehicle," United States Naval Academy Trident Scholar Project report no. 406, May 2012.

²⁴Shafer, D.M., "Active and Passive Flow Control over the Flight Deck of Small Naval Vessels," Master of Science Thesis, Aerospace Engineering Department, Virginia Polytechnic Institute and State Univ., Blacksburg, Virginia, April 2005.

ACKNOWLEDGEMENTS

This project is funded by the Office of Naval Research (Murray Snyder is Principal Investigator). Midshipman interns were funded by the Department of Defense High Performance Computing Modernization Program Office. The contributions of Ensign Jason Metzger involving remote controlled instrumented helicopters^{22,23} were particularly noteworthy.

Murray Snyder, Ph.D., P.E., a retired US Navy Captain, is a Research Professor at both George Washington University and the US Naval Academy.

Hyung Suk Kang, Ph.D., is a Researcher at the Johns Hopkins University Applied Physics Laboratory.

Cody Brownell, Ph.D., is an Assistant Professor in the Mechanical Engineering Department at the US Naval Academy.

John Burks, a former US Navy test pilot, is a Visiting Professor in the Aerospace Engineering Department at the US Naval Academy.